OPEN

PRS GLOBAL OPEN

EXPERIMENTAL

BMP-7 Preserves Surface Integrity of Degradable-ceramic Cranioplasty in a Göttingen Minipig Model

J. Camilo Roldán, MD, DMD, PhD*†
Peter Schulz, DMD‡
Tim Klünter, DMD‡
Ulrike Deisinger, PhD§
Claudius Diez, MD, PhD¶
Waltraud Waiss, MD, DMD‡
Christian Kirschneck, DMD‖
Torsten E. Reichert, MD, DMD, PhD‡
Rainer Detsch, PhD**

Background: The aim of the study was to evaluate the integrity of a craniotomy grafted site in a minipig model using different highly porous calcium phosphate ceramic scaffolds either loaded or nonloaded with bone morphogenetic protein-7 (BMP-7).
Methods: Four craniotomies with a diameter of 15 mm (critical-size defect) were grafted with different highly porous (92–94 vol%) calcium phosphate ceramics [hydroxyapatite (HA), tricalcium phosphate (TCP), and biphasic calcium phosphate (BCP; a mixture of HA and TCP)] in 10 Göttingen minipigs: (a) group I (n = 5): HA versus BCP; (b) group II (n = 5): TCP versus BCP. One scaffold of each composition was supplied with 250 µg of BMP-7. In vivo computed tomography scan and fluorochrome bone labeling were performed. Specimens were evaluated 14 weeks after surgery by environmental scanning electron microscopy, fluorescence microscopy, and Giemsa staining histology.
Results: BMP-7 significantly enhanced bone formation in TCP ($P = 0.047$). Slightly enhanced bone formation was observed in BCP ($P = 0.059$) but not in HA implants. BMP-7 enhanced ceramic degradation in TCP ($P = 0.05$) and BCP ($P = 0.05$) implants but not in HA implants. Surface integrity of grafted site was observed in all BMP-7-loaded implants after successful creeping substitution by the newly formed bone. In 9 of 10 HA implants without BMP-7, partial collapse of the implant site was observed. All TCP implants without BMP-7 collapsed. Fluorescent labeling showed bone formation at week 1 in BMP-7-stimulated implants.
Conclusions: BMP-7 supports bone formation, ceramic degradation, implant integration, and surface integrity of the grafted site. *(Plast Reconstr Surg Glob Open 2017;5:e1255; doi: 10.1097/GOX.0000000000001255; Published online 16 March 2017.)*

INTRODUCTION

Synthetic bone substitutes are very promising in bone regeneration because their availability is unlimited; they can be tailored as a patient-specific implant via *computer-aided design*. Furthermore, antigenicity or infection transmission is excluded.[1] Nevertheless, no material currently available fulfills the ideal criteria for cranial reconstruction. The newly formed bone should fully replace an implant, while the mechanical properties of the grafted area meets functional demands and the shape remains unchanged.[2] Since many years, metallic (titanium alloy), polymeric [polymethylmethacrylate (PMMA) and more recently polyetheretherketone], ceramic (calcium phosphates[3]), and bioactive glasses[4] are available for clinical use.[5] Metallic implants interfere magnetic resonance images[6]; moreover, exposition and infection are possible complications.[3] PMMA materials are predisposed to exposure because of infection, especially in large implants in irradiated tissue

*From the *Division of Pediatric Facial Plastic Surgery and Craniofacial Anomalies, Catholic Children's Hospital Wilhelmstift, Hamburg, Germany; †Teaching Hospital of the University of Lübeck, Lübeck, Germany; ‡Department of Cranio-Maxillofacial Plastic Surgery, University of Regensburg, Regensburg, Germany; §Friedrich-Baur-Research-Institute for Biomaterials, Bayreuth, Germany; ¶Department of Cardiothoracic Surgery, University of Regensburg, Regensburg, Germany; ‖Department of Orthodontics, University of Regensburg, Regensburg, Germany; and **Department of Biomaterials, Cell Biology and Tissue Engineering, University of Erlangen, Erlangen, Germany.*
Current address: Ulrike Deisinger, CeramTec GmbH, CeramTec-Platz 1, 91207 Lauf, Germany.
Received for publication August 2, 2016; accepted January 11, 2017.
Preliminary results were presented at the Conference of the European Society of Craniofacial Surgery, September 27–29, 2012, Goteborg, Sweden.

DOI: 10.1097/GOX.0000000000001255

Disclosure: *The authors have no financial interest to declare in relation to the content of this article. This study was supported by the German Ministry of Education and Research (Bundesministerium für Bildung und Forschung, BMBF), grant No. 0315019, a joint project of the Friedrich-Baur-Research Institute (Prof. G. Ziegler and Dr. Detsch), Bayreuth, and the Department of Cranio-Maxillofacial Plastic Surgery, University of Regensburg (Dr. Roldán). The Article Processing Charge was paid for by the authors.*

and in proximity to the sinuses in frontal cranioplasty.[3,7] Hydroxyapatite (HA) implants showed a limited osteointegration and limited resorption in the craniomaxillofacial area.[8] Despite the above-mentioned disadvantages, all these materials are routinely used in adults.[3] Moreover, custom-made nonresorbable implants are not suitable for children because cranial expansion cannot be restrained. Cranial bone defects in the growing infant are relatively common after cranial vault reshaping in craniosynostosis surgery. The autologous bone graft is still the *gold standard* for cranial reconstruction in children. Rib bone transplant is of limited use because this kind of bone resorbs, producing a "washboard" appearance, which is not acceptable in aesthetic regions like the forehead.[3] Cranial bone transplant seems to be more stable because cranial bone is more resistant to resorption.[9] Techniques on harvesting cranial bone grafts mark the foundation of craniofacial surgery. Tessier et al.[10] reported more than 20,000 cases in which a bone defect of the craniofacial and maxillofacial area was treated by a bone graft. Detailed information on techniques and tools for harvesting full-thickness cranial bone grafts and split cranial bone grafts for transposition and also particulate cranial bone graft for small defects was provided.[11] Despite the benefit of the autologous bone graft, the major limitation is the limited source. Bone morphogenetic proteins (BMPs) in an osteoconductive carrier showed to be valuable in craniomaxillofacial surgery.[2,12] Springer et al.[13] reported about cranial reconstruction in the growing Göttinger minipig using a collagen scaffold loaded with BMP-7. An unrestricted skull growth was observed. Nevertheless, for the repair of big cranial defects, a collagen carrier for BMP is not suitable because an anatomical implant design is not possible. Biphasic calcium phosphate (BCP) ceramics [a mixture of HA and tricalcium phosphate (TCP)] seem to be promising materials as cranial implant because the addition of TCP to HA allows remodeling via degradation.[8] Furthermore, computer-aided design technology is applicable to calcium phosphate ceramics (CPCs). The replacement of a ceramic scaffold by the newly formed bone is a critical issue, especially in craniofacial surgery, because implant geometry should remain unaltered until bone replacement takes over to meet the highly aesthetic demands of this area. The calcium phosphate composition, sintering, and pore geometry play a critical role in bone regeneration and remodeling as observed in the present ceramic in in vitro studies[14,15] and in vivo in the ectopic mouse model.[16] CPCs are suitable carriers for BMPs as demonstrated by Urist et al.[17] and Ripamonti et al.[18] among other authors.

The aim of the present study was to evaluate the effect of BMP-7 on different CPCs in a Göttinger minipig craniotomy model in terms of integrity of the implant site after ceramic creeping substitution by the newly formed bone.

MATERIALS AND METHODS

Ten adult Göttingen minipigs aged in average 36 months and weighing in average 33–41 kg (Ellengard Göttingen Minipigs ApS, Dalmose, Denmark) were operated on. The animals were fed with 2 × 250 g standard soft diet (Altromin 9023; Atronium International GmbH, Lange, Germany) and water ad libitum. The present study was approved by the local authorities for animal protection at Oberpfalz, Bavaria (No. 54-2531.1-02/07) and the Ethics Committee at the University of Regensburg, Germany. All experiments were performed at the Experimental Animal Facility at the University of Regensburg.

Experimental Procedure

The frontal bone was shaved and cleaned with povidone iodine solution and draped with sterile towels in a prone position. Five craniotomy critical-size defects with a diameter of 15 mm (Craniotome Type GA054/74; Aesculap, Tuttlingen, Germany) were set in the frontal bone, preserving the sinus mucosa at a distance of 2.5 cm from the midline and 2.5 cm from each other at the ipsilateral site (Fig. 1). Due to the maturity of the animals, the whole frontal bone was pneumatized by frontal sinus; no dura mater was exposed. Four bone defects were grafted with different highly porous CPCs [HA, TCP, and BCP (HA/TCP in a ratio of 60/40 wt% = HA60)] developed at the Friedrich-Baur-Research-Institute for Biomaterials, University of Bayreuth, Germany, not clinically available yet. The fifth defect remained ungrafted as a control defect (Fig. 1). The CPCs used had interconnecting macropores with a bimodal pore size distribution (360–440 and 900–1150 mm). The surface of the ceramic struts was microporous with pores of the size 0.4–4 μm. The total porosity of the CPCs was very high (92–94 vol%) as reported previously.[14,16,19] One scaffold of each composition was supplied with 250 μg of BMP-7 diluted in 20 mM acetate buffer with 5% mannitol (pH = 4.5), providing full embedment of the implant (generous gift from Prof. S. Vukicevic, Laboratory for Mineralized Tissues Center for Translational and Clinical Research, University of Zagreb, School of Medicine and Genera, Krapinske Toplice, Croatia). BMP-7 was supplied in situ by using a pipette (Pipette; Eppendorf Research

Fig. 1. Medial subperiosteal scalp dissection showing 5 craniotomies with a diameter of 15 mm. Two defects are localized anteriorly at 1 cm above the supraorbital foramen and a distance of 2.5 cm from the midline (below; frontal). Two more defects are placed posteriorly at 15 mm from the anterior defects (above; occipital). A lateral defect (left side in reference to the specimens) remained ungrafted as a control site. Craniotomies are grafted with different CPCs (HA, TCP, and BCP) loaded alternatively with 250 μg of BMP-7 applied in situ.

plus, Hamburg, Germany) with sterile tips. Ripamonti[20] informed about the same effect on bone formation by applying 0.1, 0.5, or 2.5 mg of BMP-7 in a craniotomy model in the adult baboons, *Papio ursinus*. Consequently, the applied doses in the present study should be appropriate. BMP-7 was selected to compare results with the authors' previous studies using the same ceramic.[14,16] Groups working on BMP-2 inform about similar results in terms of bone formation.[21]

Two animal groups were set up (each n = 5): group I: HA and BCP with and without BMP-7 (4 implants in each animal); group II: TCP and BCP with or without BMP-7 (4 implants in each animal; Fig. 2). In total, 40 implants were evaluated and compared for statistical purposes: HA (n = 5), TCP (n = 5), BCP (n = 10), HA + BMP-7 (n = 10), TCP + BMP-7 (n = 5), and BCP + BMP-7 (n = 10).

In vivo computed tomography (CT) was performed at weeks 1, 10, and 14 after surgery in intravenous anesthesia. CT was performed with a 16-slice spiral CT scanner (Siemens Somatom Plus 4/Sensation 16; Siemens, Erlangen, Germany) with the following scan parameters: 120 kV, 33 mA, and slice thickness of 1 mm. Images were analyzed on a Syngo 3D Workstation Leonardo (Siemens, Erlangen, Germany).

The parameters evaluated according to Parfitt[22] were as follows:

- Core volume = bone volume + mineralized surface (area in mm^2)
- Implant height = distance mineralized surface from implant bed to skull surface (mm)
- Implant density (HU)

An in vivo *polychrome sequential labeling* of mineralizing tissues was performed as described previously.[23,24] Sequential apposition of fluorochromes provides information about temporal bone formation in vivo. Intraperitoneal injection of fluorochromes started 1 week after the surgical procedure and continued sequentially in weeks 6, 8, and 12 after surgery as follows: xylenol orange (6% in 2% $NaHCO_3$ solution, 1.5 ml/kg body weight), calcein green (1% in 2% $NaHCO_3$ solution, 5 ml/kg body weight), alizarin complexon (3% in 2% $NaHCO_3$ solution, 0.8 ml/kg body weight), and doxycycline (1 ml/kg body weight; Ratiopharm GmbH and Co., Ulm, Germany). Images were evaluated with a fluorescent microscope using universal objective for simultaneous capture of all fluorochromes injected (BX16; Olympus, Düsseldorf, Germany). Images were analyzed with Cell P (Olympus Soft Imaging Solutions GmbH, Muenster, Germany). Selective fluorochrome evaluation and three-dimensional (3D) image analysis were performed by using a confocal laser scanning microsocope LSM 510 (Zeiss, Jena, Germany).

Animals were killed 14 weeks after surgery by an intravital and intracardial perfusion of a saline and a fixation solution [25% glutaraldehyde (2.5%), formaldehyde (1.5%), and Sörensen's phosphate buffer (100 mM KH_2PO_4, 100 mM $Na_2HPO_4 \times 2H_2O$, pH 7.4)] at 37°C and a pressure of 120 mm Hg as described previously[12,24]; a lateral thoracotomy was preferred. A mechanical pump Medos Deltastream DP2 and a Jostra Heat Exchanger HEC44 were used (Heart Technology Facility, Department of Cardiothoracic Surgery, University of Regensburg).

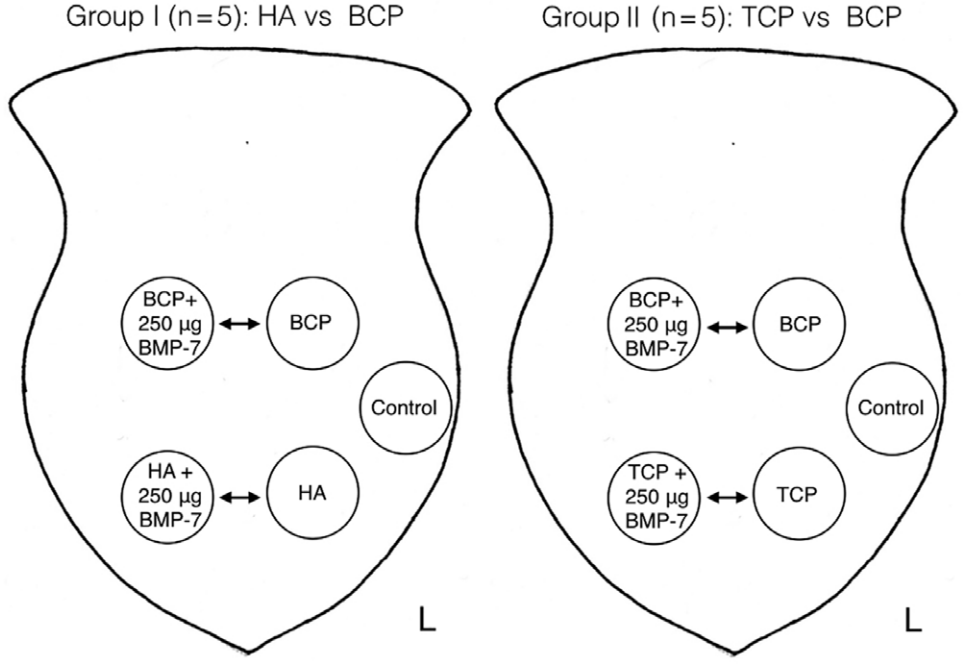

Fig. 2. Craniotomy model in the Göttingen minipig with 5 critical-size defects placed in the frontal bone. Four defects are grafted with different CPCs; the fifth defect in the left frontal bone remained empty as control. Two animal groups were set up (each n = 5). Group I: HA vs BCP with and without BMP-7. Implants were alternatively placed in the right and in the left side; Group II: TCP vs BCP with or without BMP-7.

Histology

Each sample was harvested en block and sectioned in the middle after performing an x-ray of the frontal bone. The surrounding soft tissues were preserved to avoid alteration of the implant surface (cranial implant). Explanted specimens were dehydrated in a graded series of alcohol and, subsequently, embedded in methylmethacrylate (MMA).[25] The polished surface of an MMA block was analyzed by environmental scanning electron microscopy (ESEM; Quanta 200; FEI, Hillsboro, Ore.) at 0.5–0.6 mbar and 15 kV and a magnification of ×150 as described previously.[16] The following parameters were evaluated[22] by using an imaging software analySIS Pro3.2 (Soft Imaging Systems GmbH, Muenster, Germany):

- Area of the newly mineralized bone
- Area of the ceramic (ratio evaluated in percentage)
- Integrity of the implant site is scored as collapse (yes; no) defined as follows: Collapse = shrinking of the implant site producing irregularity and depression of mineralized surface in reference to the skull surface; No collapse = surface integrity of the implant site in line with the skull profile as a result of successful creeping substitution of the implant by the newly formed bone.

An unimplanted ceramic embedded in MMA (native ceramic) was evaluated as control to evaluate ceramic gray values as a reference for ceramic degradation (dissolution or resorption) in the experimental group. Subsequently, the MMA blocks were cut, ground, and polished into sections with a thickness of 90 µm. Those sections were evaluated for fluorescence labeling[12] and then stained with Giemsa to evaluate the newly formed bone, bone marrow, and integrity of sinus mucosa.[16,26]

Statistical Analysis

The statistical analysis was done with Stata 10.1 SE for Windows (StataCorp, Inc., College Station, Tex.) and SigmaPlot 11 for Windows (SYSTST Inc., Chicago, Ill.). Graphs were created with SigmaPlot 11. Data were graphically tested for normality with Q-Q plots, followed by a formal analysis with the Shapiro-Wilk test.

Continuous, normally distributed data from more than 2 groups were compared with analysis of variance followed by pairwise comparison (Holm-Sidak). Comparison of 2 groups was done by Student's *t* test. Comparison of continuous non-normally distributed data from more than 2 groups was performed with the Kruskal-Wallis test, followed by a pairwise analysis with the Mann-Whitney test.

Data are presented as mean value ± SD. A P value < 0.05 was considered as statistically significant.

RESULTS

Animals gained 5% weight during the experimental period in average, the surgical procedure was well tolerated, and no complications were observed.

CT Data Correlated to Fluorescent Labeling and ESEM Imaging

CT data showed an increment in the *implant volume* (core volume) in the presence of BMP-7 (Fig. 3). In the absence of BMP-7, TPC ceramics were almost not detectable by week 10; a slight bone volume enhancement was observed by week 14 (Fig. 3). This observation correlates

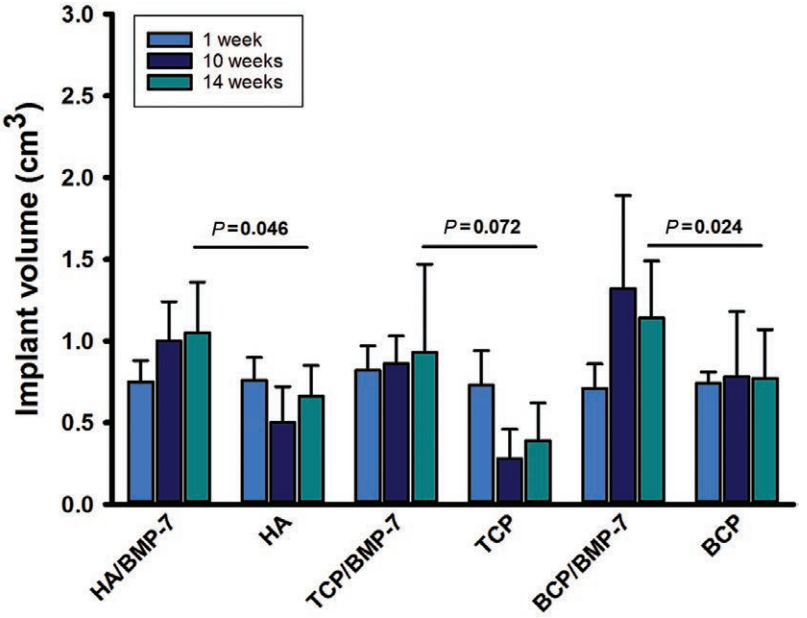

Fig. 3. Implant volume assessed in vivo by CT at weeks 1, 10, and 14. TCP ceramics drastically lost volume at week 10; some volume recovered as observed at week 14. This is explained by late bone formation, evident in fluorochrome labeling at week 10 (see also Fig. 7). BMP-7-loaded ceramics showed a statistically significant volume increment for HA and BCP ceramics (Student's *t* test after testing for normality).

with late bone formation (doxycycline marker = brown, week 12) on a collapsed TCP scaffold as observed in the fluorescent labeling (Fig. 8). The 3D CT visualization data showed a smoother surface on BMP-7-loaded implants (Fig. 4); surface irregularities in the 3D reconstruction correspond to the immature newly formed bone not detected by CT as confirmed by the ESEM imaging (Fig. 5). The control craniotomy remained unhealed, confirming the nature of the defect as a critical-size defect (Fig. 4).

Environmental Scanning Electron Microscopy

Analysis of the ESEM images by segmentation of gray values is provided in Figure 5. The newly formed bone was seen in all implants. BMP-7 enhanced bone formation in TCP (P = 0.047); a slightly enhanced bone formation was observed in BCP (P = 0.059) but not in HA implants (Fig. 6). Despite no enhanced bone formation on HA + BMP-7, slight overgrowth of bone in relation to the skull profile was observed. The implant site "expanded" because no HA degradation took place (Fig. 5, left above). BMP-7 also enhanced ceramic degradation in TCP (P = 0.05) and BCP (P = 0.05) implants but again not in HA implants (Fig. 7). The integrity of the implant site was also influenced by BMP-7. Implant site integrity (no collapse) was observed in all BMP-7-stimulated implants. In 9 of 10 HA implants without BMP-7, partial implant collapse was observed. All TCP implants without BMP-7 collapsed (Fig. 5).

Fluorescent Labeling

The fluorescent labeling showed an enhanced effect of BMP-7 on bone formation starting at week 1 (xylenol orange = orange yellow marker) in all the implants. At week 6, calcein green was observed in all specimens; nevertheless, only in BMP-7-loaded implants, homogeneous bone formation in the whole implant area was observed. In implants

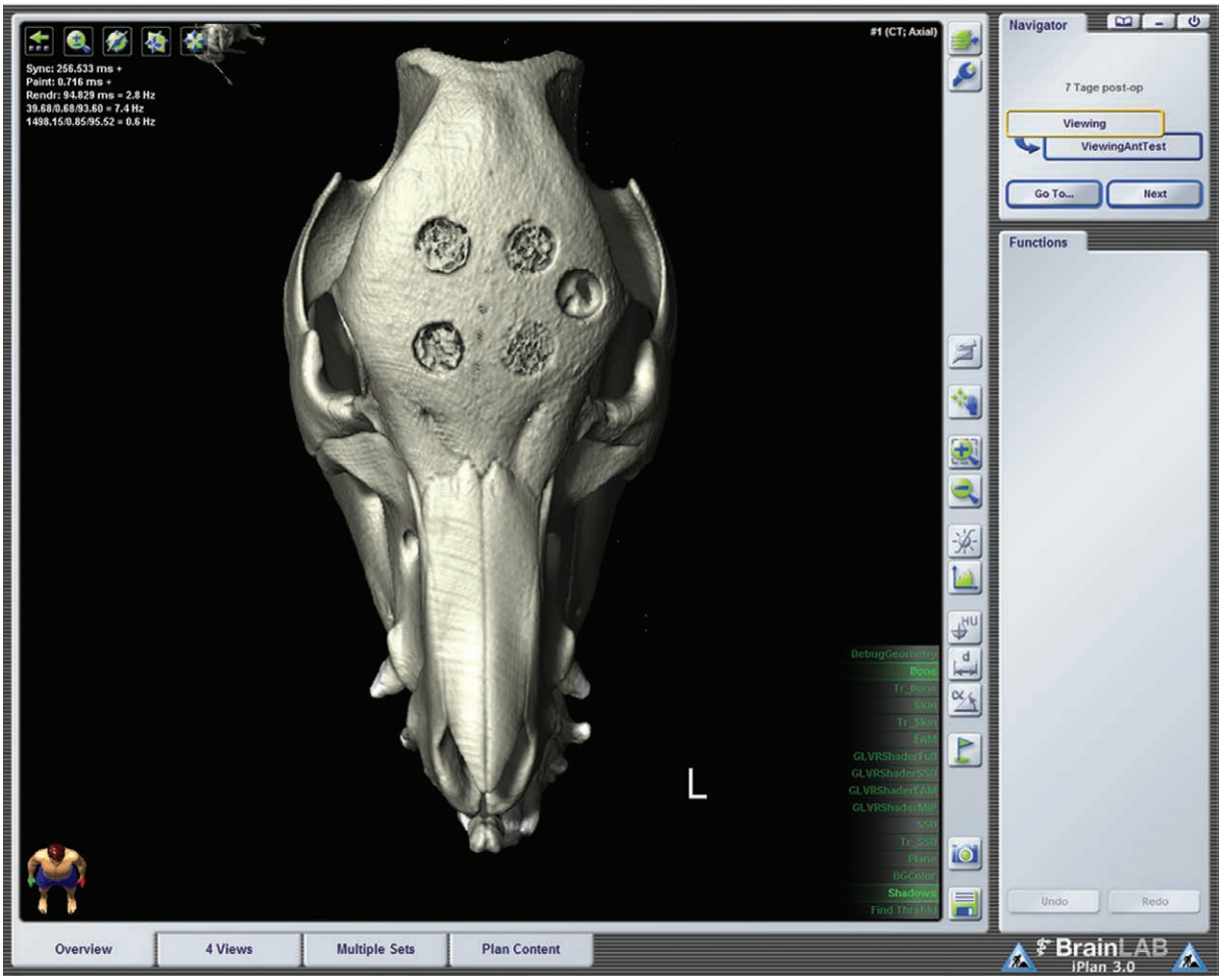

Fig. 4. In vivo 3D CT scan of the head 1 week after placement of 5 craniotomies (exemplary scan, case 1, group 1). Two anterior craniotomies were grafted with HA; 2 posterior craniotomies were grafted with BCP (the left side is grafted in the presence of BMP-7). A control craniotomy nongrafted (left side lateral) remained unhealed at the end of the study, confirming the nature of the defect as a critical-size defect. The surface continuity of grafted area differs depending on the implant composition and in the presence of BMP-7. Cranial defects loaded with BMP-7 (left) are almost repaired. Nevertheless, apparently unrepaired surface (irregularities) in the BMP-7 group is composed of the newly mineralized bone, not assessable on CT but evident on ESEM (Fig. 4). Temporary volume changes on in vivo CT are appreciated in Figure 3 (volume-rendered CT image; iPlan CMF 3; BrainLAB, Feldkirchen, Germany).

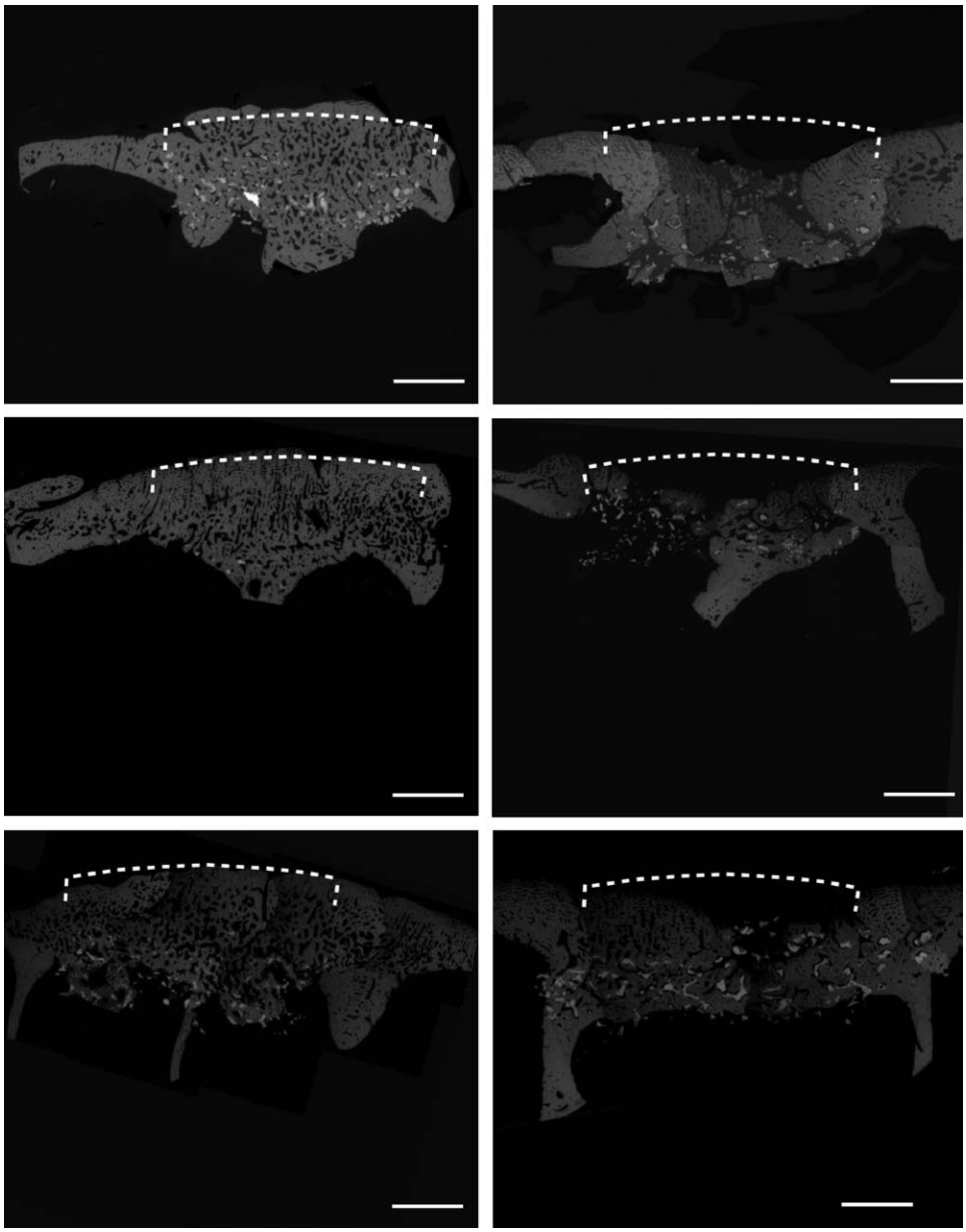

Fig. 5. ESEM images of explanted grafted frontal bone (total core). Dotted lines denote site of implant and the corresponding extension of ideal skull surface in reference to the defect border: slight overgrowth of bone on top of nondegradable HA in the presence of BMP-7 is observed (above left). HA without BMP-7 is collapsed; the newly formed bone fails to preserve the skull contour (dotted line, above right). TCP in the presence of BMP-7 is almost fully replaced by the newly formed bone. Due to fast degradation, irregularities were observed on top of the grafted area (middle row left). TCP in the absence of BMP-7 showed partial collapse (middle row right). BCP in the presence of BMP-7 showed a homogeneous bone growth; no overgrowth was observed due to advanced ceramic degradation (below left). BCP in the absence of BMP-7 is almost completely collapsed in reference to the skull profile (below right, undecalcified in MMA-embedded specimen en block analyzed, composite images, scale bar: 3.5 mm).

not loaded with BMP-7, bone formation took place in an already collapsed implant site (Fig. 8). At week 8 (alizarin complexon = red marker), bone formation was observed again homogeneously in BMP-7 implants. By week 12 (doxycycline = brown marker), a cortical-like bone was observed in the grafted site in the presence of BMP-7. In nonloaded implants, soft-tissue ingrowth in an irregular collapsed implant site was observed (Fig. 8). The total fluorescent area measured at week 12 (brown marker) was similar in all specimens (Fig. 9), but in the non-BMP-7–loaded implants, the amount of bone on a delayed bone formation in weeks 1, 6, and 8 was insufficient to repair the defect (Fig. 8).

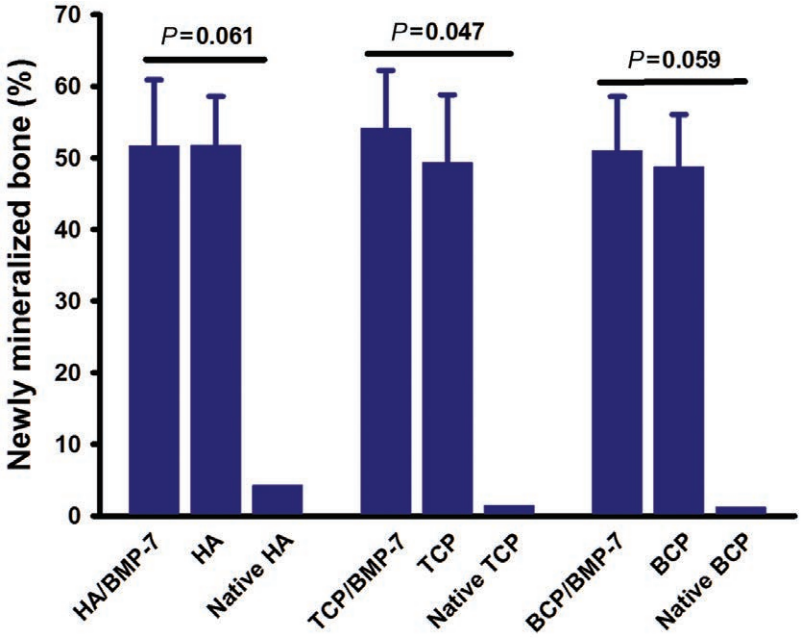

Fig. 6. Area of the newly mineralized bone assessed by ESEM. Enhanced bone formation was observed as statistically significant in TCP ceramics in the presence of BMP-7 ($P = 0.047$); a slightly enhanced bone formation was observed in BCP in the presence of BMP-7 ($P = 0.059$) but not with HA. The relative bone overgrowth in HA + BMP-7 ceramics observed in ESEM images corresponds to a bone growth shift due to the persistent ceramic occupying the defect core (Fig. 4). Nonimplanted ceramic (native ceramic) confirm that measured gray values are correctly assessed as the newly formed bone and not as ceramic (normality test Shapiro-Wilk, failed $P < 0.05$).

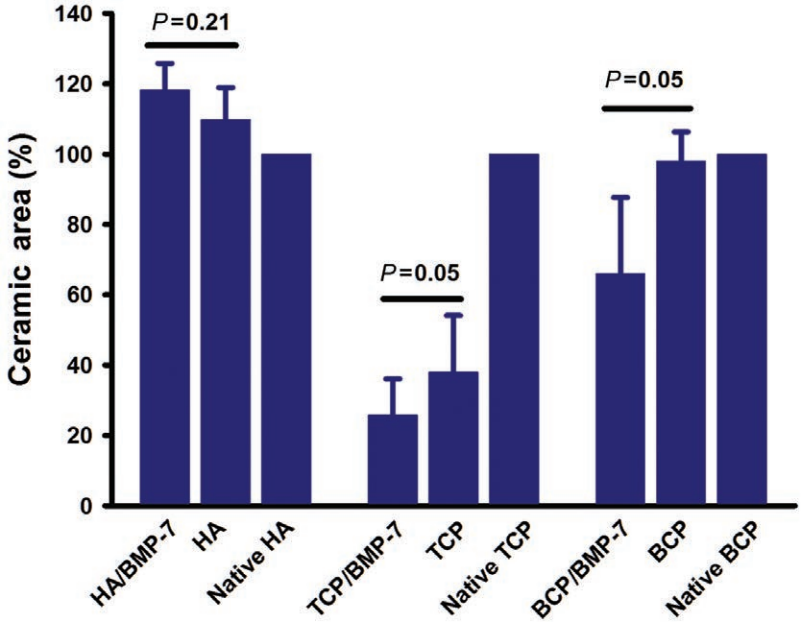

Fig. 7. Area of CPCs assessed by ESEM. BMP-7 enhanced ceramic degradation on BCP and TCP. HA remained unaltered in the presence of BMP-7; a slight enhancement of the ceramic area is explained by bone formation in the microconnective system (normality test Shapiro-Wilk, failed $P < 0.05$).

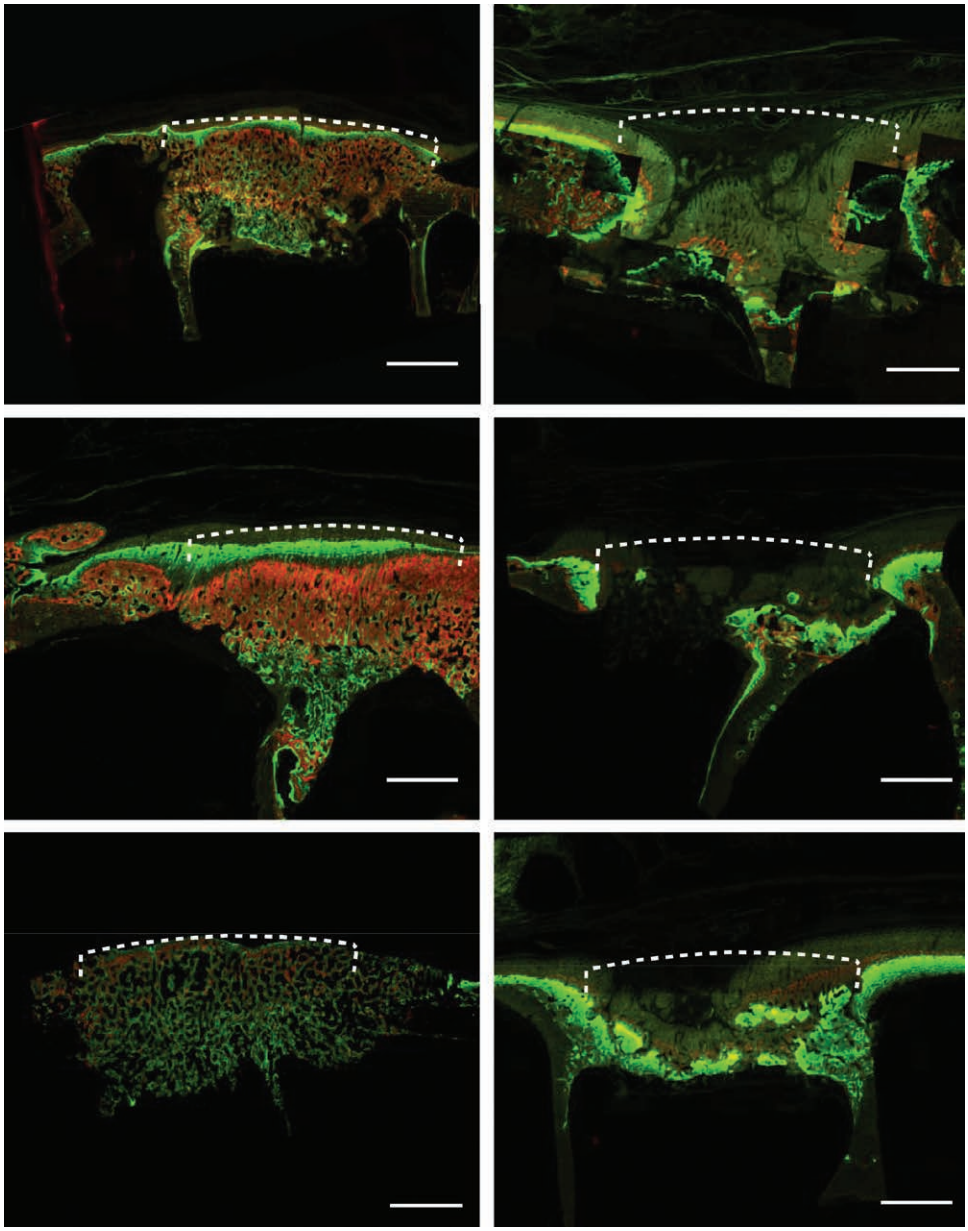

Fig. 8. Fluorochrome labeling of explanted grafted frontal bone (total core, xylenol orange/orange yellow marker at week 1; calcein green/green marker at week 6; alizarin complexon/red marker at week 8; doxycycline/brown marker at week 12). Dotted lines denote site of implant and the corresponding extension of ideal skull surface in reference to the defect border: HA is labeled starting at week 1 (orange yellow) in the presence of BMP-7. Subsequent markers are observed in sequential layers. On the top, a cortical-like bone (brown) is observed (above left). HA in the absence of BMP-7 starts bone formation at week 6 (green) in an already collapsed implant (above right). TCP in the presence of BMP-7 shows an intense fluorochrome uptake starting at week 1 (orange yellow); subsequent fluorochromes are distributed homogeneously. A cortical-like bone (brown) is observed on the top (middle row left). TCP without BMP-7 shows bone labeled at week 12 (brown). No grafted material is seen. The implant site is completely collapsed (middle row right). BCP in the presence of BMP-7 shows homogeneous bone formation, starting at week 1 (orange yellow). The implant site shows bone maturity undistinguishable from the host bone (below left). BCP without BMP-7 shows bone formation starting at week 6 (green); the implant site is already collapsed (below right, undecalcified in MMA-embedded specimen en block analyzed, composite images, scale bar: 3.5 mm).

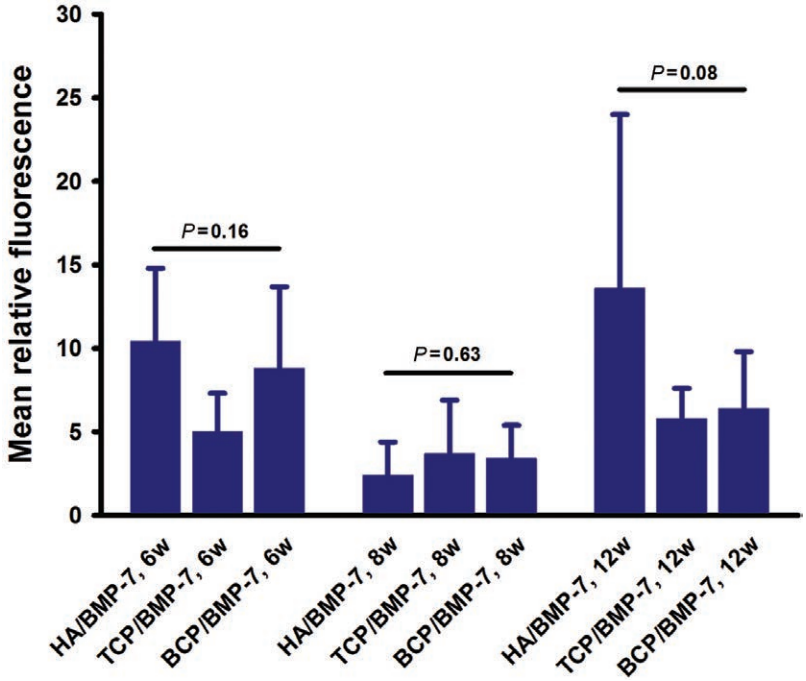

Fig. 9. Histomorphometry of fluorochromes detected at weeks 6 (green marker = calcein green), 8 (red marker = alizarin complexon), and 12 (brown marker = doxycycline). No substantial differences are observed in terms of area of the newly formed bone in the presence or not of BMP-7. Nevertheless, when late bone formation occurs as observed in implants not loaded with BMP-7, bone formation takes place in an already collapsed scaffold (Fig. 7). This result underlines the critical role of BMPs at an early stage of bone healing. An enhanced bone formation was observed in BMP-7-loaded BCP at week 6 (early bone formation); bone formation decreased at week 8 ($P = 0.01$). *P* values for intergroup comparisons are shown for 6, 8, and 12 weeks after implantation. One-way analysis of variance was used for intergroup comparisons at 6 and 8 weeks and the Kruskal-Wallis test was used for comparison at 12 weeks.

Histology

The histology in the Giemsa staining showed no inflammatory reaction in the surrounding tissues including the frontal sinus. Bone formation was observed at the surface of ceramic struts (macropores) and also inside the ceramic struts (micropores).

DISCUSSION

The beneficial effect of BMP-7 on bone formation, ceramic degradation, and creeping ceramic substitution could be proven in the presented experimental setting while the integrity of the implant surface remained unaltered.

Effect of BMP-7 on CPCs as Cranial Implants—The Integrity of the Cranial Shape

Bone formation was seen in all implants whether loaded or not with BMP-7. Nevertheless, only in the presence of BMP-7, implant site integrity (no collapse of the grafted site) was observed. In BMP-7-loaded implants, a cortical-like bone was observed in continuity to the skull profile. BMP-7 enhanced degradation of TCP and BCP ceramics by bone replacement resembling *bone remodeling* while the grafted site remained unchanged in shape. A slight bone overgrowth over skull profile was observed in HA/BMP-7 ceramics due to limited degradability of HA. Dochery-Skogh et al.[21] reported about complete degradation of a hydrogel implant in the presence of 1.25 mg of BMP-2 for cranial reconstruction in a minipig after 3 months; nevertheless, massive bone formation behind the skull profile was observed. This issue underlines the importance to characterize each implant, considering the degradability in relation to the amount of BMP applied.

Ceramics nonloaded with BMP-7 collapsed, changing skull shape. Gosain et al.[27] informed about unsuitability of CPC (HA, BCP) in the absence of BMP for augmentation of the facial skeleton (midface and frontal bone) because of unpredictable ceramic degradation, and thus unpredictable shape of skull and facial skeleton.

To overcome unpredictable cranial implant shape, Engstrand et al.[28] proposed a calcium phosphate cranial implant reinforced with a titanium mesh. Vital bone inside the mesh was observed 50 months after surgery in a follow-up study in 2 patients.[29] The titanium scaffold embedment in the newly formed bone is not removable, making the calcium phosphate implant mechanically dependent on the metallic construction. Since many years, titanium mesh has been used as a cast for bony reconstruction in the craniofacial area by using autologous bone graft or bone substitutes.[2,30] Loss of titan implants because

of infection remains a potential complication,[30] beside the limitation of MRI studies because of metallic interference.[6] The full replacement of a bone implant should be the main goal in regenerative medicine.

Enhanced Degradation of Ceramics and Bone Remodeling

In the present study, BCP and TCP scaffolds loaded with BMP-7 showed a statistically enhanced degradation after 3 months compared with scaffolds not loaded with BMP-7. This time span seems to be appropriate when considering a growing infant. Clinically, 2–3 months after craniosynostosis surgery (release of premature ossified cranial suture by bone flap at age 8 months), unrestricted skull expansion is measurable by 3D photography, despite osteosynthesis fixation with resorbable materials (personal observation). In an infant minipig craniectomy model, enhanced bone formation induced by BMP-7 in a collagen carrier showed unrestricted skull expansion as well.[13] The present ceramic combined with BMP-7 seems to be suitable for the treatment of cranial defects in the growing infant and consequently in adults.

Temporal Bone Formation Assessed by Fluorescent Labeling

In vivo data from the fluorescent labeling disclosed the pattern of bone formation. Early bone formation at week 1 (seventh day) was observed in the presence of BMP-7 in all ceramics; consequently, further appositional bone formation was undisturbed. Sato and Urist[31] described BMP-induced bone formation as an "irreversible process." Ceramics not loaded with BMP-7 showed the first fluorochrome (calcein green) at week 6; by that time, scaffolds were almost collapsed, an irreversible event for further undisturbed bone formation. Shen et al.[32] recently informed about bone formation in the mouse calvarian model by using a functionalized silk fibroin nanohydroxyapatite ceramic loaded with stromal cell–derived factor-1 and BMP-2. After initial rapid release of stromal cell–derived factor-1 in the first days, BMP-2 was released over a period of 3 weeks, showing enhanced bone formation at week 12.[32] Despite enhanced bone formation, the biofunctionalized cranial implant site showed an irregular and depressed skull surface in profile. Sustained release of bioactive factors for bone formation should be matched with the degradability and resorptive properties of the bone substitute to be used. Sustained bone formation could be appropriate for less resorbable and degradable materials as HA; nevertheless, fast degradable materials such as TCP or supplemental materials such as silk fibroin need a stronger and earlier stimulus for bone formation, as BMP does, before the bone substitute material disappears.

Ceramic Design and Composition

BCP ceramic in a ratio of 60%/40% seems to be appropriate in terms of degradability under the selected conditions. The synchronized degradability with enhanced bone formation induced by BMP-7 supports ceramic creeping substitution, avoiding collapse at the implant site. Schumacher et al.[33] evaluated *bone marrow stromal cells* on BCP 60%/40% produced by rapid prototyping technique in a static and dynamic culture. Cell differentiation was observed in both culture conditions, but cell growth and migration was enhanced in a dynamic culture.[33] The suitability of CPC to be designed via rapid prototyping technique, considering the inclusion of a wide range of interconnecting pore system,[14] makes this material promising for tailoring as a patient-specific implant, with matching effect on cellular responses and implant shape.

Because the integrity of the implant site after creeping substitution of the ceramic is of paramount importance in cranial reconstruction, mechanism of degradation (dissolution) and/or cellular digestion (osteoclast) should be clarified in the future. In preliminary studies on the present ceramic, chemical dissolution and cellular resorption of CPC could be proven in vitro.[34,35] Further in vivo studies are necessary to improve our understanding of the role of osteoclasts in ceramic digestion.

Implant Proximity to the Frontal Sinus

In the present study, the sinus mucosa was prepared and dissected from the sinus septa. In the Giemsa histology, noninflammatory infiltration was observed. The CT showed in vivo no sign of sinus involvement during the experimental period. Similar results are available for maxillary sinus elevation with different bone substitutes.[24,36] The involvement of the frontal sinus has been reported as a critical issue for PMMA cranial implants, an infection being the major cause for implant loss.[37,38] The degradability of CPC scaffolds makes them suitable for forehead reconstruction.

CONCLUSIONS

BMP-7 enhances bone formation and ceramic degradation while the grafted site remains unaltered in its integrity. Early bone formation induced by BMP supports further bone apposition throughout the scaffold. Late bone formation in nonloaded scaffolds takes place in an already collapsed grafted site. Ceramics should be characterized in terms of degradability to match the amount of BMP needed for bone enhancement, resembling an equilibrated bone remodeling system.

J. Camilo Roldán, MD, DMD, PhD
Department of Cranio-Maxillofacial Plastic Surgery
University of Regensburg
Franz-Josef-Strauß-Allee 11
93053 Regensburg, Germany
E-mail: jcamilo.roldan@yahoo.com

ACKNOWLEDGMENTS

Authors greatly thank Prof. Slobodan Vukicevic, Laboratory for Mineralized Tissues Center for Translational and Clinical Research, University of Zagreb School of Medicine, for providing us with BMP-7 and his critical evaluation of the study design and Antje Boettinger for her technical support at the Bone Research Lab at the Department of Cranio-Maxillofacial Plastic Surgery.

REFERENCES

1. Hollister SJ. Porous scaffold design for tissue engineering. *Nat Mater.* 2005;4:518–524.
2. Warnke PH, Springer IN, Wiltfang J, et al. Growth and transplantation of a custom vascularised bone graft in a man. *Lancet.* 2004;364:766–770.

3. Goodrich JT, Sandler AL, Tepper O. A review of reconstructive materials for use in craniofacial surgery bone fixation materials, bone substitutes, and distractors. *Childs Nerv Syst.* 2012;28:1577–1588.
4. Hench LL, Polak JM. Third-generation biomedical materials. *Science.* 2002;295:1014–1017.
5. Rammos CK, Cayci C, Castro-Garcia JA, et al. Patient-specific polyetheretherketone implants for repair of craniofacial defects. *J Craniofac Surg.* 2015;26:631–633.
6. Cunningham AS, Harding S, Chatfield DA, et al. Metallic neurosurgical implants for cranial reconstruction and fixation: assessment of magnetic field interactions, heating and artefacts at 3.0 Tesla. *Br J Neurosurg.* 2005;19:167–172.
7. Gosain AK; Plastic Surgery Eductional Foundation DATA Committee. Biomaterials for reconstruction of the cranial vault. *Plast Reconstr Surg.* 2005;116:663–666.
8. Gosain AK, Riordan PA, Song L, et al. A 1-year study of osteoinduction in hydroxyapatite-derived biomaterials in an adult sheep model: part II. Bioengineering implants to optimize bone replacement in reconstruction of cranial defects. *Plast Reconstr Surg.* 2004;114:1155–63; discussion 1164.
9. Greene AK, Mulliken JB, Proctor MR, et al. Primary grafting with autologous cranial particulate bone prevents osseous defects following fronto-orbital advancement. *Plast Reconstr Surg.* 2007;120:1603–1611.
10. Tessier P, Kawamoto H, Matthews D, et al. Autogenous bone grafts and bone substitutes–tools and techniques: I. A 20,000-case experience in maxillofacial and craniofacial surgery. *Plast Reconstr Surg.* 2005;116:6S–24S.
11. Tessier P, Kawamoto H, Posnick J, et al. Taking calvarial grafts–tools and techniques: VI. The splitting of a parietal bone "flap". *Plast Reconstr Surg.* 2005;116(5 suppl):74S–88S; discussion 92S.
12. Roldán JC, Jepsen S, Miller J, et al. Bone formation in the presence of platelet-rich plasma vs. bone morphogenetic protein-7. *Bone.* 2004;34:80–90.
13. Springer IN, Açil Y, Kuchenbecker S, et al. Bone graft versus BMP-7 in a critical size defect–cranioplasty in a growing infant model. *Bone.* 2005;37:563–569.
14. Roldán JC, Chang E, Kelantan M, et al. Quantifying migration and polarization of murine mesenchymal stem cells on different bone substitutes by confocal laser scanning microscopy. *J Craniomaxillofac Surg.* 2010;38:580–588.
15. Detsch R, Uhl F, Deisinger U, et al. In vitro studies of cell growth on three differently fabricated hydroxyapatite ceramic scaffolds for bone tissue engineering. *Key Eng Mater.* 2008;361–363:1181–1184.
16. Roldán JC, Detsch R, Schaefer S, et al. Bone formation and degradation of a highly porous biphasic calcium phosphate ceramic in presence of BMP-7, VEGF and mesenchymal stem cells in an ectopic mouse model. *J Craniomaxillofac Surg.* 2010;38:423–430.
17. Urist MR, Lietze A, Dawson E. [beta]-tricalcium phosphate delivery system for bone morphogenetic protein. *Clin Orthop Relat Res.* 1984;187:277.
18. Ripamonti U, Ramoshebi LN, Matsaba T, et al. Bone induction by BMPs/OPs and related family members in primates. *J Bone Joint Surg Am.* 2001;83-A(suppl 1, pt 2):S116–S127.
19. Deisinger U. *Synthetisches Knochenersatzmaterial mit spongiosa-ähnlicher Struktur.* Berlin: Mensch & Buch Verlag; 2009.
20. Ripamonti U. Bone induction by recombinant human osteogenic protein-1 (hOP-1, BMP-7) in the primate Papio ursinus with expression of mRNA of gene products of the TGF-beta superfamily. *J Cell Mol Med.* 2005;9:911–928.
21. Docherty-Skogh AC, Bergman K, Waern MJ, et al. Bone morphogenetic protein-2 delivered by hyaluronan-based hydrogel induces massive bone formation and healing of cranial defects in minipigs. *Plast Reconstr Surg.* 2010;125:1383–1392.
22. Parfitt AM. Bone histomorphometry: standardization of nomenclature, symbols and units (summary of proposed system). *Bone.* 1988;9:67–69.
23. Rahn BA. Fluorochrome labelling of bone dynamics. *Eur Cells and Mater.* 2003;5:41.
24. Roldán JC, Knueppel H, Schmidt C, et al. Single-stage sinus augmentation with cancellous iliac bone and anorganic bovine bone in the presence of platelet-rich plasma in the miniature pig. *Clin Oral Implants Res.* 2008;19:373–378.
25. Donath K, Breuner G. A method for the study of undecalcified bones and teeth with attached soft tissues. The Säge-Schliff (sawing and grinding) technique. *J Oral Pathol.* 1982;11:318–326.
26. Plenk H Jr, Shum JC, Cruise GM, et al. Cartilage and bone neoformation in rabbit carotid bifurcation aneurysms after endovascular coil embolization. *Eur Cell Mater.* 2008;16:69–79.
27. Gosain AK, Riordan PA, Song L, et al. A 1-year study of hydroxyapatite-derived biomaterials in an adult sheep model: III. Comparison with autogenous bone graft for facial augmentation. *Plast Reconstr Surg.* 2005;116:1044–1052.
28. Engstrand T, Kihlström L, Neovius E, et al. Development of a bioactive implant for repair and potential healing of cranial defects. *J Neurosurg.* 2014;120:273–277.
29. Engstrand T, Kihlström L, Lundgren K, et al. Bioceramic implant induces bone healing of cranial defects. *Plast Reconstr Surg Glob Open.* 2015;3:e491.
30. Kuttenberger JJ, Hardt N. Long-term results following reconstruction of craniofacial defects with titanium micro-mesh systems. *J Craniomaxillofac Surg.* 2001;29:75–81.
31. Sato K, Urist MR. Induced regeneration of calvaria by bone morphogenetic protein (BMP) in dogs. *Clin Orthop Relat Res.* 1985;197:301–311.
32. Shen X, Zhang Y, Gu Y, et al. Sequential and sustained release of SDF-1 and BMP-2 from silk fibroin-nanohydroxyapatite scaffold for the enhancement of bone regeneration. *Biomaterials.* 2016;106:205–216.
33. Schumacher M, Uhl F, Detsch R, et al. Static and dynamic cultivation of bone marrow stromal cells on biphasic calcium phosphate scaffolds derived from an indirect rapid prototyping technique. *J Mater Sci Mater Med.* 2010;21:3039–3048.
34. Schaefer S, Detsch R, Uhl F, et al. How degradation of calcium phosphate bone substitute materials is influenced by phase composition and porosity. *Adv Eng Mater.* 2011;13:342–350.
35. Detsch R, Boccaccini AR. The role of osteoclasts in bone tissue engineering. *J Tissue Eng Regen Med.* 2015;9:1133–1149.
36. Klongnoi B, Rupprecht S, Kessler P, et al. Influence of platelet-rich plasma on a bioglass and autogenous bone in sinus augmentation. An explorative study. *Clin Oral Implants Res.* 2006;17:312–320.
37. Marchac D, Greensmith A. Long-term experience with methylmethacrylate cranioplasty in craniofacial surgery. *J Plast Reconstr Aesthet Surg.* 2008;61:744–752; discussion 753.
38. Bello-Rojas G, Whitney M, et al. Long-term results of craniofacial implantation: a return to methyl methacrylate. *Eur J Plast Surg.* 2012;35:177–180.